

See discussions, stats, and author profiles for this publication at: <https://www.researchgate.net/publication/271387938>

"Hot" ideal tensile strength of Fe

Article · January 2015

Source: arXiv

CITATIONS
0

READS
215

9 authors, including:



Xiaoqing li
University of Leeds
118 PUBLICATIONS 3,767 CITATIONS

[SEE PROFILE](#)



Lars Bergqvist
KTH Royal Institute of Technology
111 PUBLICATIONS 5,076 CITATIONS

[SEE PROFILE](#)



Hualei Zhang
Xi'an Jiaotong University
41 PUBLICATIONS 1,375 CITATIONS

[SEE PROFILE](#)



Laszlo Szunyogh
Budapest University of Technology and Economics
367 PUBLICATIONS 8,284 CITATIONS

[SEE PROFILE](#)

“Hot” ideal tensile strength of Fe

Xiaoqing Li,^{1,*} Stephan Schönecker,^{1,†} Eszter Simon,² Lars Bergqvist,³ Hualei Zhang,^{1,4} László Szunyogh,^{2,5} Jijun Zhao,^{6,‡} Börje Johansson,^{1,7} and Levente Vitos^{1,7,8}

¹*Department of Materials Science and Engineering,*

KTH Royal Institute of Technology, Stockholm SE-10044, Sweden

²*Department of Theoretical Physics, Budapest University of Technology*

and Economics, Budafoki út 8., HU-1111 Budapest, Hungary

³*Department of Materials and Nano Physics, KTH Royal Institute of Technology, Electrum 229, Kista, SE-16440, Sweden*

⁴*Center of Microstructure Science, Frontier Institute of Science and Technology,*

Xi'an Jiaotong University, Xi'an, 710054, China

⁵*MTA-BME Condensed Matter Research Group, Budafoki út 8., HU-1111 Budapest, Hungary*

⁶*Key Laboratory of Materials Modification by Laser,*

Ion and Electron Beams (Dalian University of Technology), Ministry of Education, Dalian 116024, China

⁷*Department of Physics and Astronomy, Division of Materials Theory,*

Uppsala University, Box 516, Uppsala, SE-75120, Sweden

⁸*Research Institute for Solid State Physics and Optics,*

Wigner Research Center for Physics, Budapest HU-1525, P.O. Box 49, Hungary

(Dated: January 26, 2015)

The ideal tensile strength (ITS) of body-centered cubic (bcc) Fe is studied as a function of temperature. It is found that the ITS is only slightly temperature dependent below ~ 500 K but exhibits large thermal gradients at higher temperatures. Thermal expansion and electronic excitations have an overall moderate effect, but magnetic disorder reduces the ITS with a pronounced 90 % loss in strength in the temperature interval ~ 500 - 900 K. The effect is associated with losing the ferromagnetism upon tensile deformation. As an implication, we show that $\text{Fe}_{0.9}\text{Co}_{0.1}$ possesses a much higher ITS than Fe at temperatures above ~ 600 K due to the Co-induced strengthening of the magnetic order.

PACS numbers: 62.20.-x, 81.40.Jj, 75.50.Bb

Developing new structural materials for high-temperature services, such as power plants, pollution control, and gas turbines, is a demanding task. One of the challenges is to maintain the ambient material’s strength at elevated and high temperatures. Modeling the temperature effect on the attainable strength determined by complex micro-structural properties associated with defects like vacancies, dislocation networks, and grain boundaries, is an enormous task for *ab initio* methods. However, the ideal strength, that provides an upper bound on the strength that a material can withstand [1] and that applies to a perfect crystal lattice in the absence of defects, has been accessible to *ab initio* modeling at 0 K. Today, the ideal strength is a widely accepted intrinsic mechanical parameter of theoretical and practical importance [2–8].

The measured maximum strength of filamentary crystals (whiskers) and nanoscale systems (e.g., nanopillars) can approximate the theoretically predicted ideal strength [1, 10], as such systems can exhibit very low defect density. Iron is the basic ingredient of steels, which belong to the most important structural materials for high temperature service. Brenner measured systematically the tensile strength of bcc Fe whiskers and determined its temperature dependence [9, 11]. It was found that the maximum tensile strength of [001]-oriented Fe whiskers drops by about 67 % (the average

tensile strength drops by 60 %) as temperature increases from 298 K to 823 K (data shown in the inset of Fig. 1).

Iron orders ferromagnetically (FM) below the Curie temperature ($T_C = 1043$ K), and the paramagnetic (PM) bcc phase persists up to 1189 K [12]. Parallel to the gradual loss of magnetic long-range order strong changes of its elastic thermo-mechanical properties are observed, e.g., for the elastic anisotropy and the elastic stiffness in tension [13]. Although the ITS of Fe has been widely studied [3, 14–18], so far all efforts were limited to 0 K. Extending these investigations to high-temperatures will broaden the possibility for assessing the impact of ITS in high-temperature mechanical properties of micro-scale materials.

In this Letter, we explore the effect of finite temperatures on the ITS of bcc Fe in tension along the weakest direction ([001]) with a theoretical approach based on first-principles. We take into account three basic contributions arising from phononic, electronic and magnetic degrees of freedom. We demonstrate that in contrast to the other two effects, the change of magnetic disorder leads to a significantly ITS reduction in the temperature interval ~ 500 - 900 K. Applying our approach to the case of $\text{Fe}_{0.9}\text{Co}_{0.1}$ alloy, we show that Co substantially improves the ITS of Fe at temperature higher than 600 K.

The adopted first-principles method is based on

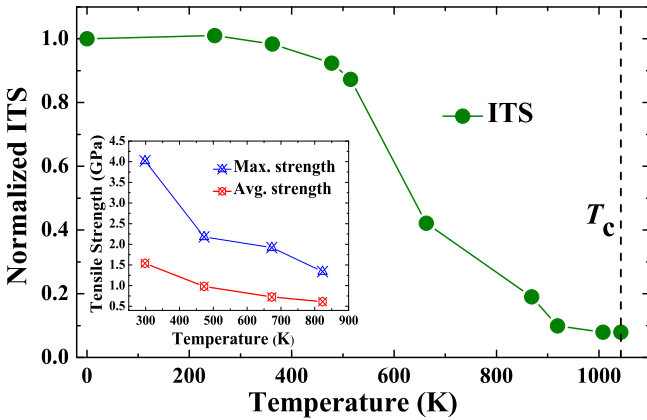


FIG. 1. (Color online) Computed ITS of bcc Fe in tension along the [001] direction as a function of temperature normalized to the ITS at 0 K (12.6 GPa). (Inset) Experimentally determined tensile strength of [001] oriented Fe whiskers as a function of temperature from Ref. 9. The two data sets give the average tensile strength and the maximum tensile strength for whiskers possessing nearly equal diameter (5.1–5.4 μm). Lines guide the eye.

density-functional theory as implemented in the exact muffin-tin orbitals (EMTO) method [19] with exchange-correlation parameterized by Perdew, Burke, and Ernzerhof (PBE) [20]. EMTO features the coherent-potential approximation (CPA), which allows to describe the disordered PM state by the disordered local moment (DLM) approach [21].

The ITS (σ_m) is the first maximum of the stress-strain curve, $\sigma(\epsilon) = \frac{1+\epsilon}{V(\epsilon)} \frac{\partial G}{\partial \epsilon}$ ($V(\epsilon)$ is the relaxed volume at strain ϵ), upon uniaxial loading. The tensile stress was determined by incrementally straining the crystal along the [001] direction and taking the derivative of the computed free energy [$G(\epsilon)$] with respect to ϵ . The two lattice vectors perpendicular to the [001] direction were relaxed at each value of the strain allowing for a possible symmetry lowering deformation with respect to the initial body-centered tetragonal symmetry (bct, lattice parameters a and c) [18]. The PBE error in the equilibrium volume was estimated to affect the ITS by less than 1 GPa at 0 K and 0.2 GPa at 1000 K.

The temperature induced contribution of electronic excitations to the ITS was considered by smearing the density of states with the Fermi-Dirac distribution [22]. The change in the ITS due to electronic excitations was found to be less than 1% at ~ 1000 K. To measure the effect of explicit lattice vibrations, we computed the vibrational free energy as a function of strain in the vicinity of the stress maximum within the Debye model [23] employing an effective Debye temperature which was determined from bulk parameters [24]. We found that explicit phonon terms decrease the ITS by approximately 5% at high temperature (663 K) and leads to an approximately

1% change at lower temperature (362 K). Both of the above effects are substantially lower than those due to the magnetic disorder and thermal expansion considered below, and thus they are not explicitly discussed here.

In order to take into account the effect of thermal expansion, the ground-state bcc lattice parameter at temperature T was obtained by rescaling the theoretical equilibrium lattice parameter with the experimentally determined thermal expansion [12]. The expanded volume was stabilized by a hydrostatic stress p_T derived from the partial derivative of the bcc total energy with respect to the volume taken at the expanded lattice parameter corresponding to T . p_T was accounted for in the relaxation during straining the lattice. To this end, the relaxed lattice maintained an isotropic normal stress p_T in the (001) plane for each value of the strain.

We modeled the effect of thermal magnetic disorder on the total energy by means of the partially disordered local moment (PDLM) approximation [25, 26]. Within PDLM, the magnetic state of Fe is described as a binary alloy $\text{Fe}_{1-x}^{\uparrow}\text{Fe}_x^{\downarrow}$ with concentration x varying from 0 to 0.5 and anti-parallel spin orientation of the two alloy components. Case $x = 0$ corresponds to the completely ordered FM state with magnetization $m = 1$. As x is gradually increased to 0.5, the magnetically random PM state lacking magnetic long and short range order ($m = 0$) is obtained (DLM state). The PDLM approach describes the energetics underlying the loss of magnetic order. Access to the temperature is provided through the magnetization curve ($m(\tau)$, $\tau \equiv T/T_C$ being the reduced temperature) which maps the computed m to the temperature T assuming T_C is known.

It is important to realize that for Fe the thermal spin dynamics embodied in the shape of $m(\tau)$ and in the T_C value change under structural deformation [27, 28]. The change in T_C under uniaxial tension was accounted for by solving the effective Heisenberg Hamiltonian, $\mathcal{H} = -1/2 \sum_{i \neq j} J_{ij} \mathbf{e}_i \cdot \mathbf{e}_j$, of classical spins \mathbf{e}_i with exchange integrals J_{ij} employing Monte Carlo (MC) simulations with the UppAsd program [29]. T_C was derived from the crossing points of the fourth order Binder cumulant [30]. Magnetization curves for Fe derived from classical MC simulations do, however, not reproduce the shape of the experimental magnetization curve at low temperatures due to the use of classical Boltzmann statistics [31, 32]. An alternative approach to $m(\tau)$, which does not suffer from this drawback, is to use the analytic expression $m_s(\tau)$ suggested by Kuz'min [33, 34]. The only free variable (s , shape parameter) in $m_s(\tau)$ is related to the spin-wave stiffness constant (D) and defined as $s = 0.1758 \frac{g\mu_B}{M_0} \left(\frac{k_B T_C}{D} \right)^{\frac{3}{2}}$ [33, 34], where g is the experimental spectroscopic splitting factor [35] and M_0 is the volume saturation magnetization. For lower than cubic symmetry, D means the geometric average of the principal values of the spin-wave stiffness tensor,

TABLE I. Magnetic quantities used to compute the shape parameter s of the bcc phases of Fe and Fe-Co at the theoretical equilibrium volume compared to the available experimental and theoretical data.

| | M_0 (kG) | g | D (meV Å 2) | T_C (K) | s |
|-------------------------------------|-------------------|-------------------|----------------------|------------------------|----------------------|
| Fe | 1.85 | 2.09 ^a | 244 | 1066 | 0.42 |
| | | | 220-287 ^b | 1015-1270 ^c | 0.41 ^d |
| Fe _{0.9} Co _{0.1} | 1.77 ^e | 2.08 ^a | 280-330 ^f | 1043 ^g | 0.35(2) ^h |
| | | | | 1148 ⁱ | |

^a Experiment; Ref. 35.

^b Refs. 34 and 40 and references therein.

^c Ref. 41 and references therein.

^d Ref. 32.

^e Experiment; Ref. 42.

^f Experiment; Refs. 43-45.

^g Experiment; Ref. 12.

^h Fit to experimental magnetization curve; Ref. 34.

ⁱ Experiment; Ref. 46.

$D = (D_x D_y D_z)^{1/3}$ [36]. Here D_α ($\alpha = x, y, z$) were computed from the exchange integrals J_{ij} in a numerically converging way [37]. The J_{ij} 's of Fe entering the MC simulations and the computation of D were obtained by means of the magnetic force theorem [38] in the FM state using the EMTO method [39].

To assess the reliability of our computational approach, we first computed the magnetic quantities M_0 , T_C , D , and s for bcc Fe [47]. Our theoretical ground state lattice parameter is $a_{\text{bcc}} = 2.834 \text{ \AA}$, which is slightly below the experimental one (2.867 \AA [48]). The present results and the available theoretical and experimental data are summarized in Table I. The PBE overbinding results in a slightly too large M_0 compared to the experimental value. The computed D and T_C of bcc Fe agree well with the previously published theoretical results, although the theoretical values for D are with the exception of Ref. 40 systematically smaller than the measured ones. The presently derived shape parameter for Fe (0.42) is in line with a previous assessment (0.41, Ref. 32), but both theoretical assessments are larger than the value fitted to the experimental magnetization curve (0.35(2) [34]). This discrepancy is mainly due to the underestimated D .

Our theoretically predicted $\sigma_m(T)$ for Fe obtained by taking into account the thermal expansion and magnetic effects, is shown in Fig. 1. Temperature has a severe impact on the ITS of Fe in the investigated temperature range. At 0 K, the ITS of Fe amounts to 12.6 GPa. It remains nearly constant up to 362 K, and decreases then by $\sim 8\%$ at temperature ~ 478 K compared to the 0 K strength. The ITS drops significantly by $\sim 90\%$ between ~ 478 K and ~ 920 K. At temperatures above ~ 1008 K, Fe fails in the PM phase with an attainable ITS of ~ 1.0 GPa. For all investigated temperatures, we

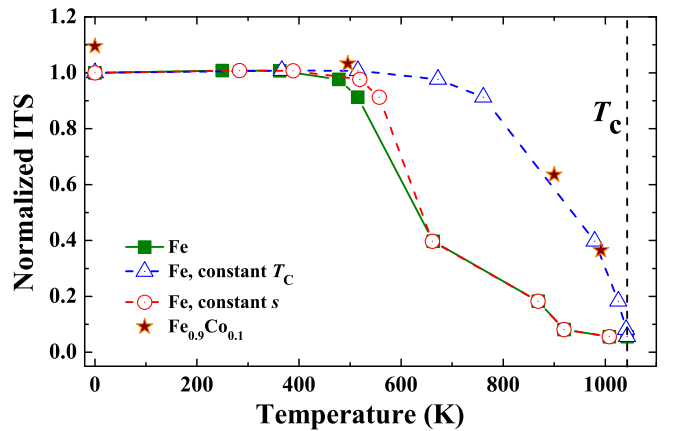


FIG. 2. (Color online) The normalized ITS of bcc Fe in tension along the [001] direction as a function of temperature taking into account only the effect of magnetic disorder (solid line); the normalized ITS when the change of T_C with structural deformation is not considered (σ_m^c , dashed line, triangles); the normalized ITS if the change of s with structural deformation is not considered (dashed line, circles). The ITS of the Fe_{0.9}Co_{0.1} alloy possesses a slightly larger ITS at 0 K but it drastically increases at high temperatures compared to pure Fe. All data is normalized to the ITS of Fe at 0 K (12.6 GPa).

found that Fe maintains bct symmetry during the tension process and eventually fails by cleavage of the (001)-planes.

In Fig. 2, we show the ITS of Fe as obtained considering merely the thermal magnetic disorder effect. Comparing these data to those in Fig 1, it can be inferred that thermal expansion has only a moderate effect on the ITS at all temperatures and the main trend of $\sigma_m(T)$ is governed by the magnetic disorder term. The pronounced drop of the ITS setting in at ~ 478 K is related to the magnetic properties of bct Fe, most importantly to its Curie temperature. The Curie temperature is shown as a function of the bct lattice parameters in Fig. 3. Compared to bcc Fe, T_C of bct Fe is strongly reduced. The main trend is that T_C decreases if the tetragonality (c/a) increases at constant volume. In order to illustrate the significance of the lattice distortion induced reduction of T_C on the ITS, we computed an auxiliary ITS [$\sigma_m^c(T)$] assuming a constant T_C for bct Fe (the shape parameters were still the ones computed previously). We chose without loss of generality the T_C of bcc Fe derived from EMTO (1066 K). The magnetic disorder effect on $\sigma_m^c(T)$ is shown in Fig. 2. The drop of the ITS is shifted to higher temperatures for $\sigma_m^c(T)$ compared to $\sigma_m(T)$. In other words, the strongly reduced Curie temperatures of the distorted bct Fe lattices compared to bcc Fe are primarily responsible for the onset of the drop of the ITS at ~ 478 K.

In contrast to T_C , we found that the shape parameter

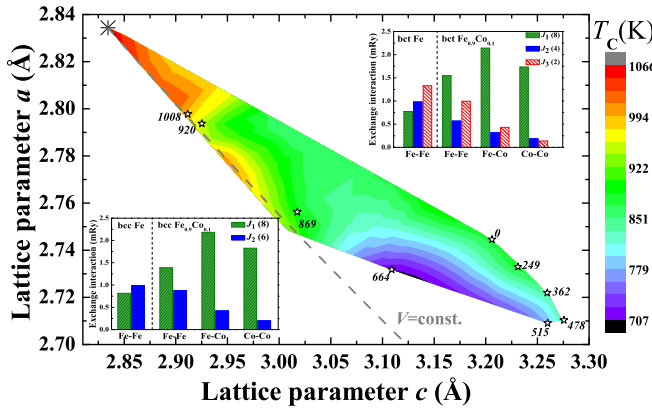


FIG. 3. (Color online) Contour plot of T_C of bct Fe as a function of the lattice parameters a and c . The region where T_C is shown is confined by the bcc ground state (black asterisk) and the failure points associated with $\sigma_m(T)$ (stars, corresponding numbers denoting T). The ground state bcc structure possesses the highest calculated T_C in the region shown. The dashed line represents the hyperbola of constant volume equal to the bcc equilibrium volume. The insets show the exchange interactions J_1 and J_2 of bcc Fe and $\text{Fe}_{0.9}\text{Co}_{0.1}$ (bottom) and $J_1\text{-}J_3$ of one representative bct structure ($a = 2.732 \text{ \AA}$, $c = 3.109 \text{ \AA}$, on top).

of bct Fe does not significantly determine $\sigma_m(T)$ (Fig. 2, open circle). Although the individual quantities T_C and D depend strongly on tetragonality and volume, both follow the same characteristic trend (the one that is displayed for T_C in Fig. 3) and their combined effect on s largely cancels out ($s \propto M_0^{-1}(T_C/D)^{3/2}$). We found that M_0 depends rather weakly on both c/a and volume.

The 0K ITS of Fe can be sensitively altered already by dilute alloying with, e.g., V or Co [18]. Apart from the intrinsic chemical effect of the solute atom, there is a magnetic effect due to the interaction between the solute atom and the Fe host. Here we show that the ITS of Fe can be significantly enhanced at high temperatures by alloying with Co.

We assessed the magnetic properties of the random $\text{Fe}_{0.9}\text{Co}_{0.1}$ solid solution using the same methodology as for Fe employing effective exchange interactions in the random alloy [38], i.e., $J_{ij} = \sum_{\alpha,\beta} c_\alpha c_\beta J_{ij}^{\alpha\beta}(c)$, where $\alpha, \beta = (\text{Fe}, \text{Co})$, $J^{\alpha\beta} = J^{\beta\alpha}$, and c is the atomic concentration. Our theoretical data for bcc $\text{Fe}_{0.9}\text{Co}_{0.1}$ ($a_{\text{bcc}} = 2.848 \text{ \AA}$) listed in Table I confirms the experimentally determined increase in T_C of dilute bcc Fe-Co alloy. We found that alloying Fe with 10% Co stiffens D by approximately 17%. This alloying effect of Co on T_C is mainly connected to the strengthening of the first nearest neighbor exchange interactions (J_1) [49, 50]. We show the influence of Co on the eight first ($J_1(8)$) and six second ($J_2(6)$) nearest neighbor exchange interactions in the inset of Fig. 3 for the bcc phase. J_1 between both similar and dissimilar atomic species increases significantly

in $\text{Fe}_{0.9}\text{Co}_{0.1}$ compared to J_1 in pure Fe. At the same time, alloying with Co weakens J_2 , but this effect is of lesser importance for T_C than the strengthening of J_1 .

Following the same procedure as described for Fe, we computed the ITS of the $\text{Fe}_{0.9}\text{Co}_{0.1}$ alloy at 0K [18] and in the high-temperature interval between 496K and 1000K. As shown in Fig. 2, $\text{Fe}_{0.9}\text{Co}_{0.1}$ exhibits a $\sim 10\%$ larger ITS than Fe at temperatures below 500K, but the impact of alloying on the ITS is especially dramatic in the high-temperature region. The physical origin underlying this effect is the higher Curie temperature of bct $\text{Fe}_{0.9}\text{Co}_{0.1}$ compared to bcc Fe, which is a result of both the enhanced nearest neighbor exchange interactions and the stronger ferromagnetism in $\text{Fe}_{0.9}\text{Co}_{0.1}$, i.e., both the magnetic moment and exchange interactions are larger and more stable in the Fe-Co alloy than in pure Fe upon structural perturbation (tetragonalization) [18, 50, 51]. The alloying effect of Co on $J_1(8)$, $J_2(4)$, and $J_3(2)$ (the two third nearest neighbor interactions) is shown in Fig. 3 for one representative bct structure (with $a = 2.732 \text{ \AA}$ and $c = 3.109 \text{ \AA}$, on top). The influence of Co is a strong increase of J_1 and a weakening of J_2 and J_3 similar to the behavior of Co in the bcc phase. For the chosen example, the T_{CS} of Fe and $\text{Fe}_{0.9}\text{Co}_{0.1}$ amount to 707K and 1053K, respectively, i.e., Co addition results in an increase of T_C which is in magnitude much more pronounced for the bct structure than the impact of Co alloying for the bcc phase.

The predicted strong dependence of $\sigma_m(T)$ above $\sim 500\text{K}$ should be observable in flawless systems for which whiskers are good approximants. For single-crystalline Fe whiskers tensioned along [001] [9, 11], Brenner determined a pronounced temperature dependence of the average and maximum tensile strengths as shown in Fig. 1 (presumably, the maximum strength corresponds to whiskers with the lowest defect density and highest surface perfection). The failure of whiskers with diameter $< 6\mu\text{m}$ were reported to occur without appreciable plastic deformation. Moreover, the observed temperature gradient of the measured strength is stronger than the one assuming only the thermally-activated nucleation of dislocations at local defects [9]. On the other hand, the present results show a strong temperature gradient (mainly due to magnetic disorder) that is nicely reflected in the experimental data. The qualitative difference in the theoretical and experimental temperature dependence may be ascribed to the low strain-rate inherent in experiment, which allows for the activation of various mechanisms (dislocation activation, nucleation, etc.) not considered in the theory [52–54]. We suggest to measure the ITS of Fe-Co whiskers at elevated temperatures to investigate the predicted difference in the ITS between Fe and $\text{Fe}_{0.9}\text{Co}_{0.1}$. The output of such experiments could also be used to verify the connection between the ITS and the measured tensile strength of single-crystalline whiskers.

In summary, we showed that the ITS of Fe along the [001] direction is not significantly temperature dependent below ~ 500 K, however, diminishes significantly in the temperature interval $\sim 500 - 900$ K due to the loss of the net magnetization upon uniaxial strain. The ITS in the paramagnetic bcc phase is over 10 times lower than that in the ferromagnetic bcc phase. Thermal expansion and electronic smearing are found to have a moderate and very small effect, respectively. Fe fails by cleavage at all investigated temperatures. The ITS of Fe at high temperatures can be significantly enhanced by alloying with Co.

We thank E. K. Delczeg-Czirjak, M. D. Kuz'min, A. Ruban, and L. Udvardi for helpful discussions. The Swedish Research Council, the Swedish Steel Producers' Association, the European Research Council, the China Scholarship Council and the Hungarian Scientific Research Fund (research project OTKA 84078 and 109570), and the National Magnetic Confinement Fusion Program of China (2011GB108007) are acknowledged for financial support. L.B. acknowledges financial support from the Swedish e-Science Research Centre (SeRC) and Göran Gustafsson Foundation. The computations were performed using resources provided by the Swedish National Infrastructure for Computing (SNIC) at the National Supercomputer Centre in Linköping. L.S. was supported by the European Union, cofinanced by the European Social Fund, in the framework of the TÁMOP 4.2.4.A/2-11-1-2012-0001 National Excellence Program

-
- * xiaoqli@kth.se
 † stesch@kth.se
 ‡ zhaojj@dlut.edu.cn
- [1] A. Kelly and N. H. Macmillan, *Strong solids*, 3rd ed. (Clarendon Press, Oxford, 1986).
 - [2] C. Jiang and S. G. Srinivasan, *Nature* **496**, 339 (2013).
 - [3] D. M. Clatterbuck, D. C. Chrzan, and J. W. Morris, Jr., *Acta Mater.* **51**, 2271 (2003).
 - [4] S. H. Jhi, S. G. Louie, M. L. Cohen, and J. W. Morris, Jr., *Phys. Rev. Lett.* **87**, 075503 (2001).
 - [5] T. S. Li, J. W. Morris, Jr., N. Nagasako, S. Kuramoto, and D. C. Chrzan, *Phys. Rev. Lett.* **98**, 105503 (2007).
 - [6] L. Qi and D. C. Chrzan, *Phys. Rev. Lett.* **112**, 115503 (2014).
 - [7] R. Thomson, in *Solid State Physics*, Vol. 39, edited by H. Ehrenreich and D. Turnbull (Academic Press, New York, 1986) p. 1.
 - [8] M. J. Jokl, V. Vitek, and C. J. McMahon, *Acta Metall.* **28**, 1479 (1980).
 - [9] S. Bush, ed., "Fiber composite materials," (American Society for Metals, Metals Park, Ohio, 1965) Chap. 2. Factors influencing the strength of whiskers.
 - [10] A. M. Minor, S. A. S. Asif, Z. Shan, E. A. Stach, E. Cyrankowski, T. J. Wyrobek, and O. L. Warren, *Nat. Mater.* **5**, 697 (2006).
 - [11] S. S. Brenner, *J. Appl. Phys.* **27**, 1484 (1956); R. H. Doremus, B. W. Roberts, and D. Turnbull, eds., "Growth and perfection of crystals," (Wiley, New York, 1958) Chap. Properties of whiskers, pp. 157–190.
 - [12] Z. S. Basinski, W. Hume-Rothery, and A. L. Sutton, *Proc. R. Soc. Lond. A* **229**, 459 (1955); F. C. Nix and D. MacNair, *Phys. Rev.* **60**, 597 (1941).
 - [13] J. A. Rayne and B. S. Chandrasekhar, *Phys. Rev.* **122**, 1714 (1961).
 - [14] M. Černý and J. Pokluda, *Phys. Rev. B* **76**, 024115 (2007).
 - [15] M. Šob, M. Friák, D. Legut, J. Fiala, and V. Vitek, *Mat. Sci. Eng. A* **387-389**, 148 (2004).
 - [16] M. Černý, P. Šesták, J. Pokluda, and M. Šob, *Phys. Rev. B* **87**, 014117 (2013).
 - [17] M. Černý and J. Pokluda, *Phys. Rev. B* **82**, 174106 (2010).
 - [18] X. Q. Li, S. Schönecker, J. J. Zhao, B. Johansson, and L. Vitos, *Phys. Rev. B* **90**, 024201 (2014).
 - [19] O. K. Andersen, O. Jepsen, and G. Krier, in *Lectures on Methods of Electronic Structure Calculations*, edited by V. Kumar, O. K. Andersen, and A. Mookerjee (World Scientific, Singapore, 1994) p. 63; L. Vitos, *Phys. Rev. B* **64**, 014107 (2001); L. Vitos, H. L. Skriver, B. Johansson, and J. Kollár, *Comput. Mater. Sci.* **18**, 24 (2000).
 - [20] J. P. Perdew, K. Burke, and M. Ernzerhof, *Phys. Rev. Lett.* **77**, 3865 (1996); **78**, 1396 (1997).
 - [21] B. L. Gyorffy, A. J. Pindor, J. Staunton, G. M. Stocks, and H. Winter, *J. Phys. F: Met. Phys.* **15**, 1337 (1985).
 - [22] K. Wildberger, P. Lang, R. Zeller, and P. H. Dederichs, *Phys. Rev. B* **52**, 11502 (1995).
 - [23] G. Grimvall, *Thermophysical Properties of Materials* (North-Holland, Amsterdam, 1999).
 - [24] V. L. Moruzzi, J. F. Janak, and K. Schwarz, *Phys. Rev. B* **37**, 790 (1988).
 - [25] S. Khmelevskyi, I. Turek, and P. Mohn, *Phys. Rev. Lett.* **91**, 037201 (2003).
 - [26] V. I. Razumovskiy, A. V. Ruban, and P. A. Korzhavyi, *Phys. Rev. Lett.* **107**, 205504 (2011).
 - [27] F. Körmann, A. Dick, T. Hickel, and J. Neugebauer, *Phys. Rev. B* **79**, 184406 (2009).
 - [28] J. T. Wang, D. S. Wang, and Y. Kawazoe, *Appl. Phys. Lett.* **88**, 132513 (2006).
 - [29] B. Skubic, J. Hellsvik, L. Nordström, and O. Eriksson, *J. Phys.: Condens. Matter* **20**, 315203 (2008).
 - [30] D. Landau and K. Binder, *Guide to Monte Carlo Simulations in Statistical Physics* (Cambridge University Press, Port Chester, NY, USA, 2000).
 - [31] N. M. Rosengaard and B. Johansson, *Phys. Rev. B* **55**, 14975 (1997).
 - [32] F. Körmann, A. Dick, B. Grabowski, B. Hallstedt, T. Hickel, and J. Neugebauer, *Phys. Rev. B* **78**, 033102 (2008).
 - [33] M. D. Kuz'min, *Phys. Rev. Lett.* **94**, 107204 (2005).
 - [34] M. D. Kuz'min, M. Richter, and A. N. Yaresko, *Phys. Rev. B* **73**, 100401(R) (2006).
 - [35] R. A. Reck and D. L. Fry, *Phys. Rev.* **184**, 492 (1969).
 - [36] C. Herring and C. Kittel, *Phys. Rev.* **81**, 869 (1951).
 - [37] We applied the regularization procedure suggested in M. Pajda, J. Kudrnovský, I. Turek, V. Drchal, and P. Bruno, *Phys. Rev. B* **64**, 174402 (2001) to compute D . We evaluated the numerical accuracy of this method to 2 meV \AA^2 related to the choice of the damping parameter.
 - [38] I. Liechtenstein, M. I. Katsnelson, V. Antropov, and

- V. Gubanov, J. Magn. Magn. Mater **67**, 65 (1987).
- [39] In order to check our data, the spin-cluster expansion as implemented in a Screened Korringa-Kohn-Rostoker method (L. Szunyogh, L. Udvardi, J. Jackson, U. Nowak, and R. Chantrell, Phys. Rev. B **83**, 024401 (2011)) and the local spin density approximation was also used to determine the exchange integrals in the PM state. Both routes gave similar results for $\sigma_m(T)$.
- [40] A. Szilva, M. Costa, A. Bergman, L. Szunyogh, L. Nordström, and O. Eriksson, Phys. Rev. Lett. **111**, 127204 (2013).
- [41] S. V. Halilov, H. Eschrig, A. Y. Perlov, and P. M. Oppeneer, Phys. Rev. B **58**, 293 (1998).
- [42] M. B. Stearns, in *Landolt-Börnstein-Group III Condensed Matter: Numerical Data and Functional Relationships in Science and Technology*, Vol. 19a, edited by H. P. J. Wijn (Springer, Berlin, 1986).
- [43] R. Pauthenet, J. Appl. Phys. **53**, 2029 (1982); **53**, 8187 (1982).
- [44] G. Shirane, V. J. Minkiewicz, and R. Nathans, J. Appl. Phys. **39**, 383 (1968).
- [45] C. K. Loong, J. M. Carpenter, J. W. Lynn, R. A. Robinson, and H. A. Mook, J. Appl. Phys. **55**, 1895 (1984).
- [46] H. Stuart and N. Ridley, J. Phys. D **2**, 485 (1969).
- [47] The convergence of all numerical parameters and particularly the k -integration mesh was carefully checked. J_{ij} parameters for all pairs with interatomic distance $\lesssim 8a$ were computed and used for the computation of D . All J_{ij} parameters $\lesssim 5a$ were considered in the MC simulations where the largest simulation box was $30 \times 30 \times 30$ in terms of the conventional unit cell.
- [48] P. Villars and L. D. Calvert, *Pearson's handbook of crystallographic data for intermetallic phases*, 2nd ed., Vol. 4 (ASM international, Materials Park, Ohio, 1991).
- [49] C. Takahashi, M. Ogura, and H. Akai, J. Phys. Condens. Matter **19**, 365233 (2007).
- [50] M. Ležaić, P. Mavropoulos, and S. Blügel, Appl. Phys. Lett. **90**, 082504 (2007).
- [51] W. Pepperhoff and M. Acet, *Constitution and Magnetism of Iron and its Alloys* (Springer, Berlin, 2010).
- [52] T. Zhu, J. Li, A. Samanta, A. Leach, and K. Gall, Phys. Rev. Lett. **100**, 025502 (2008).
- [53] Y. Fan, Y. N. Ossetsky, S. Yip, and B. Yildiz, Phys. Rev. Lett. **109**, 135503 (2012).
- [54] Y. Fan, Y. N. Ossetsky, S. Yip, and B. Yildiz, P. Natl. Acad. Sci. USA **44**, 17756 (2013).